BIOCHEMISTRY
including biophysical chemistry & molecular biology
Article

Biochemistry **2010,** *49,* 4821–4826 4821
DOI: 10.1021/bi1005859

The Carboxyl-Terminal Segment of Apolipoprotein A-V Undergoes a Lipid-Induced Conformational Change†

Kasuen Mauldin,‡,§ Brian L. Lee,∥ Marta Oleszczuk,∥ Brian D. Sykes,∥ and Robert O. Ryan*,‡,§

‡*Center for Prevention of Obesity, Cardiovascular Disease and Diabetes, Children's Hospital Oakland Research Institute, 5700 Martin Luther King Jr. Way, Oakland, California 94609,* §*Department of Nutritional Sciences and Toxicology, University of California, Berkeley, California 94720, and* ∥*Department of Biochemistry, School of Molecular and Systems Medicine, 347 Medical Science Building, University of Alberta, Edmonton, Alberta, Canada T6G 2H7*

Received April 16, 2010; Revised Manuscript Received May 12, 2010

ABSTRACT: Apolipoprotein (apo) A-V is a 343-residue, multidomain protein that plays an important role in regulation of plasma triglyceride homeostasis. Primary sequence analysis revealed a unique tetraproline sequence (Pro293−Pro296) near the carboxyl terminus of the protein. A peptide corresponding to the 48-residue segment beyond the tetraproline motif was generated from a recombinant apoA-V precursor wherein Pro295 was replaced by Met. Cyanogen bromide cleavage of the precursor protein, followed by negative affinity chromatography, yielded a purified peptide. Nondenaturing polyacrylamide gel electrophoresis verified that apoA-V(296−343) solubilizes phospholipid vesicles, forming a relatively heterogeneous population of reconstituted high-density lipoprotein with Stokes' diameters >17 nm. At the same time, apoA-V(296−343) failed to bind a spherical lipoprotein substrate *in vitro*. Far-UV circular dichroism spectroscopy revealed the peptide is unstructured in buffer yet adopts significant α-helical secondary structure in the presence of the lipid mimetic solvent trifluoroethanol (TFE; 50% v/v). Heteronuclear multidemensional NMR spectroscopy experiments were conducted with uniformly ^{15}N- and ^{15}N/^{13}C-labeled peptide in 50% TFE. Peptide backbone assignment and secondary structure prediction using TALOS+ reveal the peptide adopts α-helix secondary structure from residues 309 to 334. In TFE, apoA-V(296−343) adopts an extended amphipathic α-helix, consistent with a role in lipoprotein binding as a component of full-length apoA-V.

Apolipoprotein (apo)[1] A-V was discovered in 2001 in a comparative genomics study (*1*) and as an mRNA upregulated during rat liver regeneration (*2*). Subsequent research has shown that apoA-V serves as a potent modulator of plasma triacylglycerol (TG) homeostasis. Mature apoA-V is a nonglycosylated protein comprised of 343 amino acids. An interesting feature of apoA-V is the presence of four consecutive Pro near the carboxyl (C) terminus (Pro293−Pro296). Indeed, this sequence element in apoA-V is conserved across species including human, rat, mouse, olive baboon, cow, wild boar, and dog but not frog or chicken. Whereas the 47-residue segment C-terminal to the tetraproline sequence in human apoA-V was postulated to comprise an independent structural domain, guanidine hydrochloride denaturation studies showed this segment comprises part of a larger C-terminal domain (*3*). A recombinant C-terminal truncated apoA-V, missing the region beyond residue 292, displayed defective lipid binding activity compared to full-length apoA-V. Furthermore, in the absence of a C-terminal domain, the N-terminal domain of apoA-V (residues 1−146) loses its capacity to bind larger lipoprotein substrates, such as very low density lipoprotein (*4*). When taken together with observations that naturally occurring C-terminal truncated apoA-V mutants in humans are associated with severe hypertriglyceridemia (HTG) (*5*, *6*), it is conceivable that residues 296−343 of apoA-V are required for proper functioning of this protein. In the present study, we have designed a protocol for expression and purification of recombinant of apoA-V(296−343). Structure−function analyses reveal unique lipid-binding properties of this peptide while heteronuclear multidimensional NMR studies provide evidence that, although apoA-V(296−343) is unstructured in buffer alone, it adopts α-helix secondary structure in a lipid mimetic environment.

EXPERIMENTAL PROCEDURES

Preparation of apoA-V(296−343). Site-directed mutagenesis was performed with the QuikChange II XL site-directed mutagenesis kit (Strategene) on an N-terminal His tag-containing human apoA-V construct encoding residues 148−343. Primers were designed to mutate the sole naturally occurring Met at position 253 (numbering corresponds to sequence position in mature, full-length apoA-V) to Ile and Pro295 to Met. Introduction of the desired mutations was verified by DNA sequencing. The variant apoA-V(148−343) was cloned into pET20b+ vector, and unlabeled, uniformly ^{15}N-labeled, or double ^{15}N/^{13}C-labeled variant apoA-V(148−343) were expressed in *Escherichia coli* BL21 cells cultured in NCZYM (unlabeled protein) or M9 minimal media (isotopically labeled protein) and purified as described previously for full-length recombinant apoA-V (*7*). Purified variant apoA-V(148−343) was then solubilized in 80% formic

†This work was supported by NIH Grant HL 073061 to R.O.R. and CIHR Grant FRN 33769 to B.D.S.

*To whom correspondence should be addressed. E-mail: rryan@chori.org. Tel: 510-450-7645. Fax: 510-450-7910.

[1]Abbreviations: apo, apolipoprotein; TG, triacylglycerol; HTG, hypertriglyceridemia; rHDL, reconstituted high-density lipoprotein; DMPC, dimyristoylphosphatidylcholine; LDL, low-density lipoprotein; PL-C, phospholipase C; CD, circular dichroism; TFE, trifluoroethanol; HSPG, heparan sulfate proteoglycan; NMR, nuclear magnetic resonance spectroscopy; HSQC, heteronuclear single-quantum correlation NMR spectrum; NOESY, nuclear Overhauser effect NMR spectroscopy; DSS, 2,2-dimethyl-2-silapentane-5-sulfonate.

Published on Web 05/14/2010

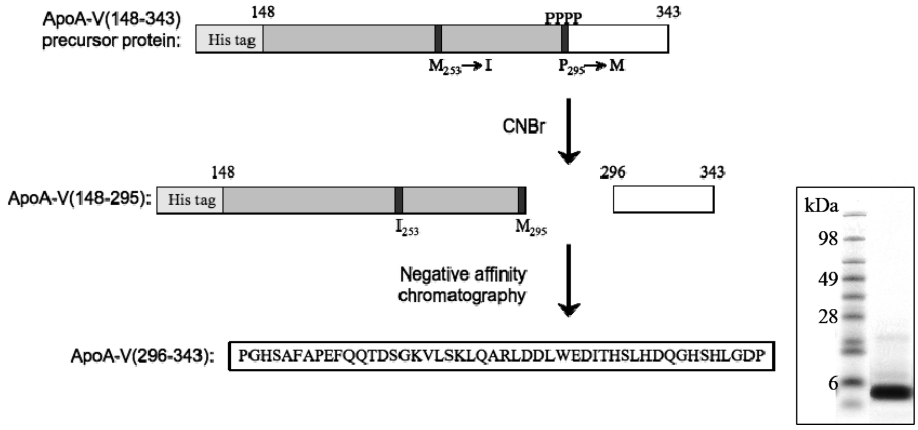

FIGURE 1: Flow chart of the apoA-V(296−343) production method and SDS−PAGE of peptide purity.

acid at a concentration of 5 mg/mL. CNBr was added at a CNBr: Met ratio >100 and incubated under N_2 atmosphere for 24 h in the dark. The reaction was quenched by addition of >10-fold excess deionized water and the sample lyophilized to remove residual CNBr. The freeze-dried product was resuspended and subjected to affinity chromatography on a Hi-Trap Ni^{2+} chelation column. Since only the unreacted variant apoA-V(148−343) substrate and the N-terminal CNBr cleavage product, apoA-V(148−295), possess a His tag, apoA-V(296−343) elutes in the unbound fraction free of contamination.

Analytical Procedures. Protein concentration in samples was determined with the bicinchoninic acid assay (Pierce) using bovine serum albumin as standard. SDS−PAGE was performed on 4−12% acrylamide slab gels using the NuPAGE MES buffer system (Invitrogen) at a constant 200 V for 35 min. Gels were stained with Gel Code Blue (Pierce). Mass spectrometry was performed on an Applied Biosystems Voyager System 6322. The matrix used was α-cyano-4-hydroxycinnamic, and the matrix and sample were dissolved in 1:1 water:acetonitrile (0.1% TFA) and drop cast.

Preparation of apoA-V(296−343) Reconstituted High-Density Lipoprotein (rHDL). Bilayer vesicles of dimyristoylphosphatidylcholine (DMPC) were prepared as described (*7*) and incubated in the presence of apoA-V(296−343) at a DMPC: peptide weight ratio of 3:1. Following bath sonication at 24 °C, the complexes generated were characterized by nondenaturing gradient polyacrylamide gel electrophoresis as described by Nichols et al. (*8*).

Low-Density Lipoprotein (LDL) Binding Assay. Human LDL (Intracel) was incubated for 90 min at 37 °C in the presence or absence of *Bacillus cereus* phospholipase C (PL-C) (0.6 unit/50 μg of LDL protein). Where indicated, apoA-V(296−343) or recombinant human apoA-I (*9*) was included in the reaction mixture (50 μg/50 μg of LDL protein). Incubations were conducted in 50 mM Tris-HCl, pH 7.5, 150 mM NaCl, and 2 mM $CaCl_2$ in a total sample volume of 200 μL. Sample turbidity was measured at 340 nm on a Spectramax 340 microtiter plate reader (Sunnyvale, CA) (*10*).

Far-UV Circular Dichroism (CD) Spectroscopy. Far-UV CD spectroscopy measurements were performed on an AVIV 410 spectrometer. Scans were obtained between 195 and 245 nm in 10 mM sodium phosphate, pH 7.4, using a protein concentration of 0.5 mg/mL.

Nuclear Magnetic Resonance (NMR) Spectroscopy. NMR experiments were performed on 1.5 mM samples of uniformly ^{15}N- or $^{15}N/^{13}C$-labeled apoA-V(296−343) in 500 μL of NMR buffer (90% H_2O/10% D_2O containing 90 mM KCl, 9 mM imidazole, and 0.5 mM 2,2-dimethyl-2-silapentane-5-sulfonate (DSS-d_6) as an internal chemical shift reference) without and with 50% trifluoroethanol (TFE-d_3). NMR experiments were carried out at 25 °C on Varian INOVA 500, 600, and 800 MHz NMR spectrometers. Data were processed using NMRPipe (*11*) and analyzed with NMRView (*12*). Sequential assignment of the backbone atoms of apoA-V(296−343) was obtained using 2D ^1H-^{15}N-HSQC, 3D ^{15}N-edited NOESY (75 ms mix), HNHA, HNCACB, and CBCA(CO)NNH experiments. 2D ^{13}C-HSQC, 3D H(CCO)NH, C(CO)NNH, and ^{13}C-edited NOESY (100 ms mix) experiments provided side-chain assignments. Secondary structure predictions were obtained using the program TALOS+ (*13*).

RESULTS

Isolation of Purified apoA-V(296−343) Peptide. Due to the size of the peptide under investigation (48 amino acids) and a desire to generate isotopically enriched apoA-V(296−343), a protocol was established to generate recombinant peptide from a larger, apoA-V(148−343) precursor. Site-directed mutagenesis was performed to replace the sole Met in this fragment with Ile, while a second mutagenesis introduced Met in place of Pro295. As predicted, CNBr cleavage of the resulting variant apoA-V(148−343) yielded two major fragments. Negative affinity chromatography was performed to isolate the peptide from unreacted precursor protein and the apoA-V(148−295) CNBr reaction product (Figure 1). One liter of culture media yielded ∼2 mg of high-purity peptide.

apoA-V(296−343) Reconstituted High-Density Lipoproteins. Incubation of apoA-V(296−343) with bilayer vesicles of DMPC induced rapid clearing of solution turbidity, indicative of rHDL formation. Native PAGE analysis revealed a relatively heterogeneous population of particles with a Stokes' diameter >17 nm (Figure 2). The rHDL generated in this reaction are larger in size than discoidal particles formed with full-length apoA-V.

apoA-V(296−343) Lipoprotein Binding Properties. When isolated human LDL is incubated with PL-C, conversion of phophatidylcholine to diacylglycerol induces lipoprotein particle instability, aggregation, and sample turbidity development (Figure 3). In control incubations lacking PL-C, no change in LDL sample turbidity was observed. When conducted in the presence of apoA-I, LDL was protected from PL-C induced aggregation and turbidity development as a result of apoA-I association with

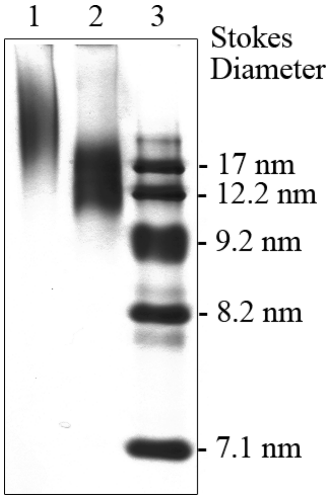

FIGURE 2: Native PAGE of apoA-V(296−343)·DMPC complexes. ApoA-V(296−343)·DMPC complexes were prepared as described under Experimental Procedures and applied to a 4−20% acrylamide gradient gel. Following electrophoresis the gel was stained with Gel Code Blue. Lane 1, apoA-V(296−343)·DMPC complexes (5 μg of protein); lane 2, full-length apoA-V·DMPC complexes (5 μg of protein); lane 3, molecular size standards.

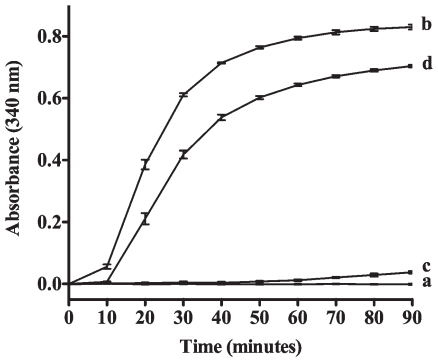

FIGURE 3: Effect of apoA-V(296−343) and apoA-I on PL-C-induced aggregation of human LDL. Human LDL (50 μg of protein) was incubated at 37 °C in the absence (curve a) or presence (curve b) of PL-C (0.6 unit). Other incubations contained LDL, PL-C, and 50 μg of apoA-V(296−343) peptide (curve d) or 50 μg of apoA-I (curve c). Sample absorbance at 340 nm was measured as a function of time. The values reported are the mean ± standard deviation (n = 3).

the modified particle surface (*10*). By contrast, corresponding incubations with apoA-V(296−343) failed to protect LDL from PL-C-induced sample turbidity development.

Far-UV CD Spectroscopy. Far-UV CD spectroscopy analysis indicates apoA-V(296−343) is largely unstructured in buffer (Figure 4). In the presence of the lipid mimetic cosolvent, TFE (50% v/v), however, major minima at 208 and 222 nm are present, indicative of α-helix secondary structure. The far-UV CD spectrum of apoA-V(296−343)·DMPC complexes is similar to that of apoA-V(296−343) in TFE (data not shown).

NMR of ^{15}N-Labeled apoA-V(296−343). When bacteria used to express the variant apoA-V(148−343) were cultured in M9 minimal media containing ^{15}N as the sole nitrogen source, uniformly ^{15}N-labeled apoA-V(296−343) was generated. Mass spectrometry analysis of the sample yielded a value of 5388 Da, in good agreement with the expected theoretical calculated mass for a fully ^{15}N-enriched peptide (5387.7 Da). NMR spectra were collected in buffer, the detergent dodecylphosphocholine (DPC), and the lipid mimetic cosolvent TFE. Comparison revealed the

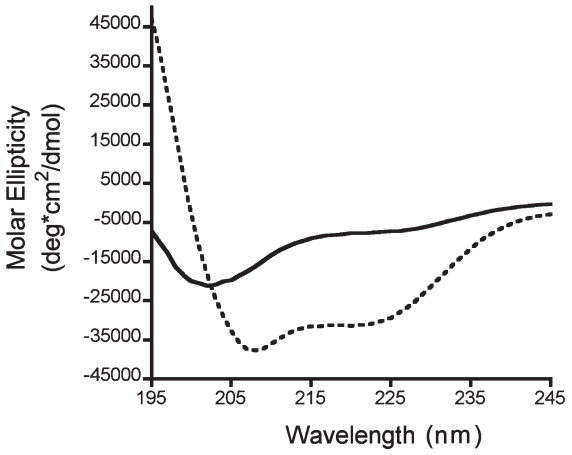

FIGURE 4: Far-UV CD of 0.5 mg/mL apoA-V(296−343) in 10 mM sodium phosphate, pH 7.4 (solid line), and in 50% TFE (dashed line).

spectra were best resolved in TFE. Thus, assignment and structure calculation were performed under this condition. Two-dimensional ^{15}N−^{1}H correlation spectroscopy of ^{15}N-labelded apoA-V(296−343) in NMR buffer gave rise to a spectrum that showed poor resonance dispersion, consistent with a general lack of secondary structure under these conditions (Figure 5a). By contrast, spectra recorded in 50% NMR buffer/50% TFE displayed significantly increased chemical shift dispersion, consistent with adoption of secondary structure (Figure 5b). Given the prospect of assigning these resonances and ultimate structure determination, a second apoA-V(296−343) peptide, enriched in both ^{15}N and ^{13}C, was generated. Using a panel of heteronuclear multidimensional NMR experiments, the backbone and side-chain atoms of apoA-V were assigned. As seen in Figure 5b, all resonances, except for G297, H298, S338, and H339, which were not visible in the ^{15}N−^{1}H HSQC, have been assigned. Secondary chemical shift values (defined as the difference between the measured chemical shift of a given atom and the corresponding chemical shift value for the same atom in random coil conformation) for ^{13}C′, ^{13}Cα, ^{13}Cβ, Hα, HN, and/or ^{15}N atoms characterize probability of helical or β-sheet conformation occurrence. The TALOS+ program (*13*) uses available secondary chemical shifts to calculate random coil index (RCI) and predict secondary structure (*14*). Positive RCI values show probable β-sheet occurrence while negative values indicate helical conformation. Prediction of the secondary structure using TALOS+ indicated peptide residues 309−334 adopt α-helix under these experimental conditions (Figure 6).

DISCUSSION

The mechanism whereby apoA-V influences plasma TG homeostasis has been the subject of intensive investigation (*15*, *16*). Studies have revealed that this protein associates with plasma lipoproteins and possesses the capacity to bind cell surface molecules including heparan sulfate proteoglycans (HSPG), members of the LDL receptor family, and glycosylphosphatidylinositol high-density lipoprotein binding protein 1 (*15*). Considering evidence from genetically engineered mouse models and population studies investigating correlations between common single nucleotide polymorphisms in *APOAV* and elevated plasma TG, better understanding of apoA-V structure and function relations may lead to new strategies to treat HTG. The fact that apoA-V concentration in plasma is extremely low (~100 ng/mL) suggests it possesses potent biological activity (*17*).

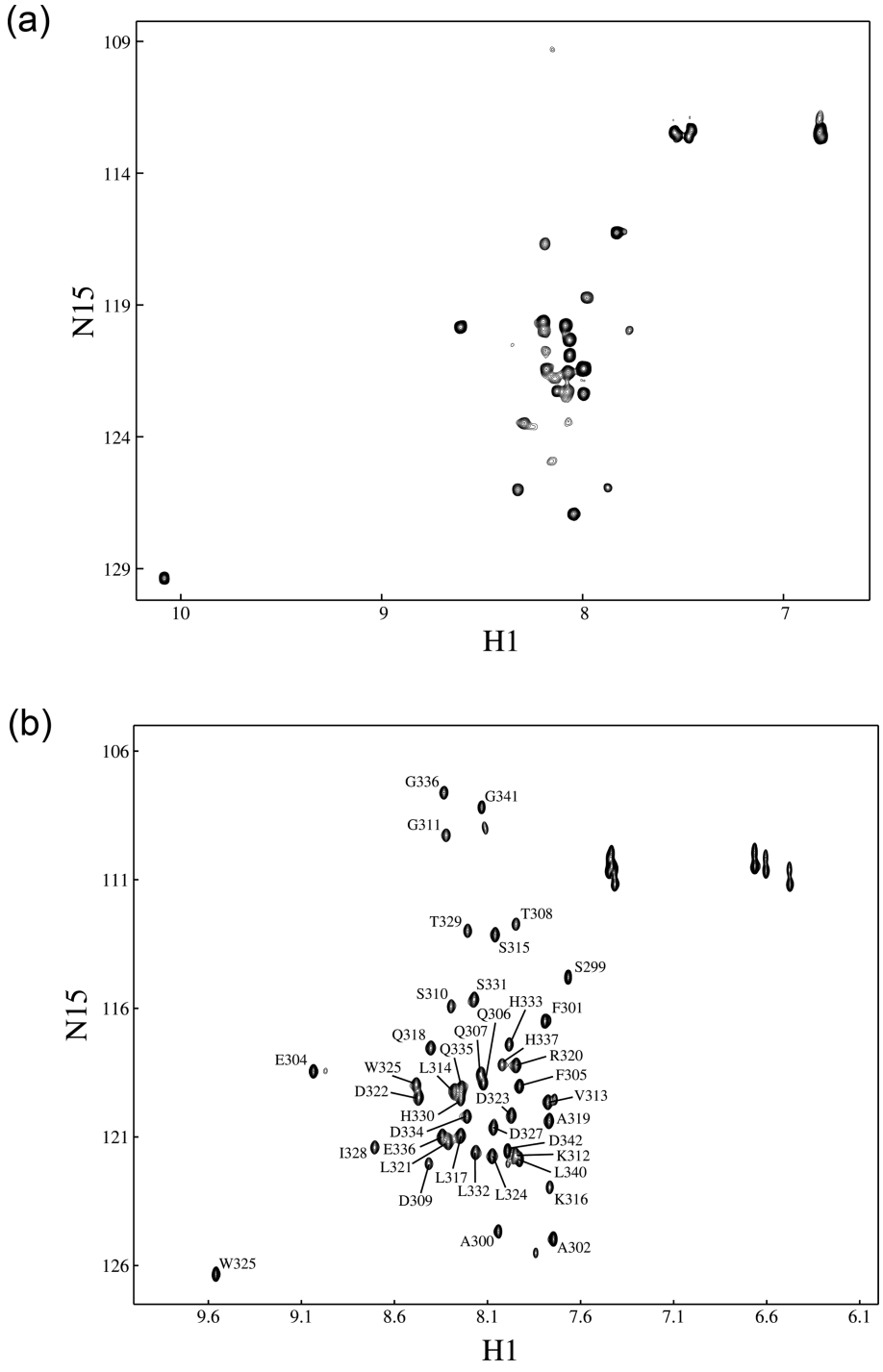

FIGURE 5: (a) 2D $^{1}H-^{15}N$ HSQC of ^{15}N-labeled apoA-V(296−343) in NMR buffer acquired at 500 MHz. (b) 2D $^{1}H-^{15}N$ HSQC of ^{15}N-labeled apoA-V(296−343) in 50% NMR buffer/50% TFE acquired at 800 MHz. Peak assignments are indicated.

Limited proteolysis and denaturation studies reveal apoA-V is comprised of two independently folded structural domains (*18*). The N-terminal domain, comprising residues 1−146, adopts a helix bundle molecular architecture in the absence of lipid (*18*). The C-terminal domain, comprising residues 147−343, is less well understood but is known to contain a sequence element (residues 186−227) that is rich in positively charged amino acids and lacks negatively charged residues. It has been postulated that this region of the protein is responsible for apoA-V interactions with cell surface proteins and HSPG (*19*−*21*).

In lipid binding studies, while the peptide corresponding to apoA-V(296−343) displays high phospholipid vesicle solubilization activity and undergoes a 16 nm blue shift in wavelength of maximum tryptophan fluorescence emission (arising from the single Trp at sequence position 325) in the presence of phospholipid (*3*), it fails to associate with the surface of a spherical lipoprotein substrate. This result illustrates important differences between lipoprotein binding and vesicle solubilization activity. The ability of apolipoproteins to bind PL-C-treated LDL is dependent on creation of binding sites, via PL-C-mediated conversion of phosphatidylcholine to diacylglycerol, whereas interaction with phospholipid bilayer vesicles proceeds optimally at the phospholipid gel to liquid-crystal phase transition temperature (*22*). It appears that the lack of secondary structure in buffer

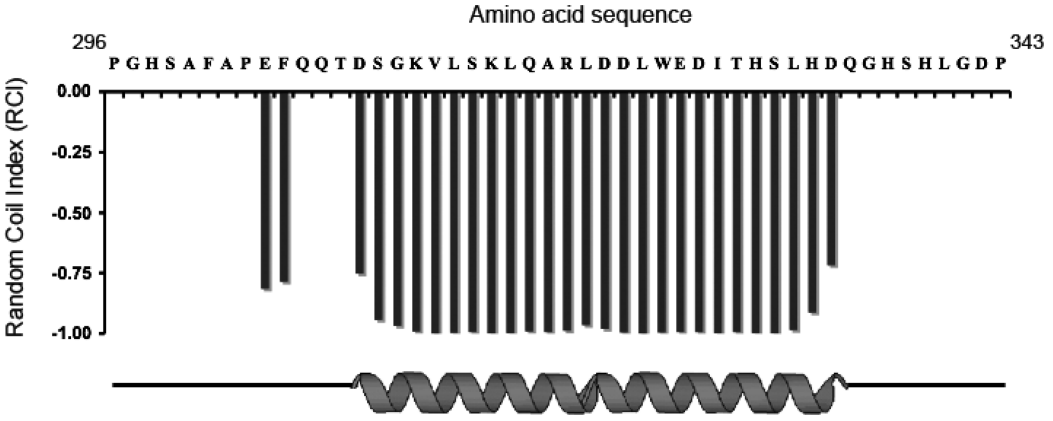

FIGURE 6: Secondary structure prediction using the TALOS+ program. Residues G297, H298, S338, and H339 could not be assigned and are not predicted.

precludes recognition/binding to the surface of a lipoprotein yet its intrinsic capacity to associate with lipid is retained in the phospholipid vesicle solubilization assay, perhaps owing to the induction of secondary structure as part of the solubilization reaction.

A concept that has emerged from structural studies conducted to date is that the C-terminal segment beyond the four consecutive Pro may be responsible for initiation of apoA-V lipid binding activity. This interpretation is consistent with the lipid binding properties of other apolipoproteins, such as apoE and apoA-I (*23*), and is supported by data showing that removal of this C-terminal region results in an impaired ability of apoA-V to bind lipid (*3*). It may be postulated that initiation of lipid binding is mediated by hydrophobic interactions between nonpolar residues in the C-terminal peptide and the hydrophobic lipid surface and/or ionic interactions between charged residues and phospholipid headgroups. In both types of interactions, the C-terminal peptide may be envisioned to mediate initial recognition of the lipoprotein particle, followed by stable binding of the entire protein.

The experiments described in this study indicate that in order to initiate lipid binding, apoA-V(296−343) may need to exist within the context of the intact protein. Far-UV CD and NMR spectroscopy experiments show that apoA-V(296−343) is unstructured in buffer alone. In the case of other apolipoproteins, adoption of a more loosely folded structure correlates with enhanced lipid binding activity (*24*). It is conceivable the C-terminal region of apoA-V initiates lipid binding and that this process induces stable secondary structure formation in this segment of the protein. In this case, it seems plausible that lipid binding elicits a subsequent conformational change in the N-terminal helix bundle that results in opening of the bundle and exposure of its hydrophobic interior to potential lipid interaction sites. A consequence of this may also include exposure of the positively charged sequence motif (residues 186−227) that underlies the biological effects of apoA-V.

In an effort to test hypotheses related to this model, we sought to characterize the structural properties of the C-terminal peptide. In order to study the peptide in isolation, methods were developed to produce recombinant peptide. Using this system, efficient stable isotope enrichment of the peptide was readily achieved. A panel of heteronuclear multidimensional NMR experiments was employed to assign the apoA-V(296−343) spectrum and define its structure in a lipid mimetic environment. Results obtained suggest apoA-V(296−343) undergoes a lipid-induced conformational change, transitioning from an unstructured or molten globule-like state in the lipid-free environment to α-helix in a lipid mimetic environment. NMR analysis reveals the region between residues 309−334 adopts a α-helix secondary structure under these conditions. These data confirm the prediction from the Coils program (*25*) that the region between Gly311 and Leu332 in apoA-V(296−343) adopts α-helical secondary structure. Edmundson helical wheel projection (*26*) of Gly311−Ile328 reveals this region forms an amphipathic α-helix with clearly demarcated polar and nonpolar faces. Primary sequence analysis reveals almost all of the hydrophobic and charged residues within apoA-V(296−343) reside within this α-helix segment. Thus, it may be considered that, in the presence of lipid, the extreme carboxyl terminus of apoA-V adopts an amphipathic α-helix. This induction of structure supports the concept that the C-terminal region of apoA-V may serve as a lipid sensor that functions in initiation of full-length apoA-V lipid binding activity and subsequent structure conformation changes in the entire protein, as seen with apoE and apoA-I (*23*). The known ability of apoA-V to transfer between high-density lipoprotein and very low density lipoprotein suggests the present findings are physiologically relevant (*4*, *27*).

Since our data show apoA-V C-terminal peptide can adopt structure, it must be considered that, when present in the context of the intact protein, the C-terminal region possesses a more defined structure. Indeed, an important question arising from this study relates to whether the C-terminal peptide structure determined here resembles that of the peptide when present in the context of the intact protein. To determine this, expressed protein ligation represents a potential strategy to generate a segmentally isotope-labeled full-length apoA-V wherein only residues 296−343 are enriched with stable isotope (*28*). Such an approach would allow detailed analysis of the solution properties and lipid binding induced conformational changes in this region of the protein within the context of the intact apoA-V protein.

ACKNOWLEDGMENT

The authors thank Dr. Clayton Mauldin of the University of California, Berkeley, for assistance with mass spectrometry analysis and Dr. Susan Marqusee of the University of California, Berkeley, for access to the circular dichroism spectrophotometer.

REFERENCES

1. Pennacchio, L. A., Olivier, M., Hubacek, J. A., Cohen, J. C., Cox, D. R., Fruchart, J. C., Krauss, R. M., and Rubin, E. M. (2001) An apolipoprotein influencing triglycerides in humans and mice revealed by comparative sequencing. *Science 294*, 169–173.

2. van der Vliet, H. N., Sammels, M. G., Leegwater, A. C., Levels, J. H., Reitsma, P. H., Boers, W., and Chamuleau, R. A. (2001) Apolipoprotein A-V: a novel apolipoprotein associated with an early phase of liver regeneration. *J. Biol. Chem. 276*, 44512–44520.
3. Beckstead, J. A., Wong, K., Gupta, V., Wan, C. P., Cook, V. R., Weinberg, R. B., Weers, P. M., and Ryan, R. O. (2007) The C terminus of apolipoprotein A-V modulates lipid-binding activity. *J. Biol. Chem. 282*, 15484–15489.
4. Wong-Mauldin, K., Raussens, V., Forte, T. M., and Ryan, R. O. (2009) Apolipoprotein A-V N-terminal domain lipid interaction properties in vitro explain the hypertriglyceridemic phenotype associated with natural truncation mutants. *J. Biol. Chem. 284*, 33369–33376.
5. Marcais, C., Verges, B., Charriere, S., Pruneta, V., Merlin, M., Billon, S., Perrot, L., Drai, J., Sassolas, A., Pennacchio, L. A., Fruchart-Najib, J., Fruchart, J. C., Durlach, V., and Moulin, P. (2005) Apoa5 Q139X truncation predisposes to late-onset hyperchylomicronemia due to lipoprotein lipase impairment. *J. Clin. Invest. 115*, 2862–2869.
6. Oliva, C. P., Pisciotta, L., Li Volti, G., Sambataro, M. P., Cantafora, A., Bellocchio, A., Catapano, A., Tarugi, P., Bertolini, S., and Calandra, S. (2005) Inherited apolipoprotein A-V deficiency in severe hypertriglyceridemia. *Arterioscler., Thromb. Vasc. Biol. 25*, 411–417.
7. Beckstead, J. A., Oda, M. N., Martin, D. D., Forte, T. M., Bielicki, J. K., Berger, T., Luty, R., Kay, C. M., and Ryan, R. O. (2003) Structure-function studies of human apolipoprotein A-V: a regulator of plasma lipid homeostasis. *Biochemistry 42*, 9416–9423.
8. Nichols, A. V., Krauss, R. M., and Musliner, T. A. (1986) Nondenaturing polyacrylamide gradient gel electrophoresis. *Methods Enzymol. 128*, 417–431.
9. Ryan, R. O., Forte, T. M., and Oda, M. N. (2003) Optimized bacterial expression of human apolipoprotein A-I. *Protein Expression Purif. 27*, 98–103.
10. Liu, H., Scraba, D. G., and Ryan, R. O. (1993) Prevention of phospholipase-C induced aggregation of low density lipoprotein by amphipathic apolipoproteins. *FEBS Lett. 316*, 27–33.
11. Delaglio, F., Grzesiek, S., Vuister, G. W., Zhu, G., Pfeifer, J., and Bax, A. (1995) NMRPipe: a multidimensional spectral processing system based on UNIX pipes. *J. Biomol. NMR 6*, 277–293.
12. Johnson, B. A., and Blevins, R. A. (1994) NMRView: a computer porgram for the visualization and analysis of NMR data. *J. Biomol. NMR 4*, 603–614.
13. Shen, Y., Delaglio, F., Cornilescu, G., and Bax, A. (2009) TALOS+: a hybrid method for predicting protein backbone torsion angles from NMR chemical shifts. *J. Biomol. NMR 44*, 213–223.
14. Berjanskii, M. V., and Wishart, D. S. (2008) Application of the random coil index to studying protein flexibility. *J. Biomol. NMR 40*, 31–48.
15. Forte, T. M., Shu, X., and Ryan, R. O. (2009) The ins (cell) and outs (plasma) of apolipoprotein A-V. *J. Lipid Res. 50* (Suppl.), S150–S155.
16. Wong, K., and Ryan, R. O. (2007) Characterization of apolipoprotein A-V structure and mode of plasma triacylglycerol regulation. *Curr. Opin. Lipidol. 18*, 319–324.
17. O'Brien, P. J., Alborn, W. E., Sloan, J. H., Ulmer, M., Boodhoo, A., Knierman, M. D., Schultze, A. E., and Konrad, R. J. (2005) The novel apolipoprotein A5 is present in human serum, is associated with VLDL, HDL, and chylomicrons, and circulates at very low concentrations compared with other apolipoproteins. *Clin. Chem. 51*, 351–359.
18. Wong, K., Beckstead, J. A., Lee, D., Weers, P. M., Guigard, E., Kay, C. M., and Ryan, R. O. (2008) The N-terminus of apolipoprotein A-V adopts a helix bundle molecular architecture. *Biochemistry 47*, 8768–8774.
19. Lookene, A., Beckstead, J. A., Nilsson, S., Olivecrona, G., and Ryan, R. O. (2005) Apolipoprotein A-V-heparin interactions: implications for plasma lipoprotein metabolism. *J. Biol. Chem. 280*, 25383–25387.
20. Merkel, M., Loeffler, B., Kluger, M., Fabig, N., Geppert, G., Pennacchio, L. A., Laatsch, A., and Heeren, J. (2005) Apolipoprotein AV accelerates plasma hydrolysis of triglyceride-rich lipoproteins by interaction with proteoglycan-bound lipoprotein lipase. *J. Biol. Chem. 280*, 21553–21560.
21. Nilsson, S. K., Lookene, A., Beckstead, J. A., Gliemann, J., Ryan, R. O., and Olivecrona, G. (2007) Apolipoprotein A-V interaction with members of the low density lipoprotein receptor gene family. *Biochemistry 46*, 3896–3904.
22. Narayanaswami, V., Wang, J., Kay, C. M., Scraba, D. G., and Ryan, R. O. (1996) Disulfide bond engineering to monitor conformational opening of apolipophorin III during lipid binding. *J. Biol. Chem. 271*, 26855–26862.
23. Saito, H., Lund-Katz, S., and Phillips, M. C. (2004) Contributions of domain structure and lipid interaction to the functionality of exchangeable human apolipoproteins. *Prog. Lipid Res. 43*, 350–380.
24. Soulages, J. L., and Bendavid, O. J. (1998) The lipid binding activity of the exchangeable apolipoprotein apolipophorin-III correlates with the formation of a partially folded conformation. *Biochemistry 37*, 10203–10210.
25. Lupas, A., Van Dyke, M., and Stock, J. (1991) Predicting coiled coils from protein sequences. *Science 252*, 1162–1164.
26. Schiffer, M., and Edmundson, A. B. (1967) Use of helical wheels to represent the structures of proteins and to identify segments with helical potential. *Biophys. J. 7*, 121–135.
27. Nelbach, L., Shu, X., Konrad, R. J., Ryan, R. O., and Forte, T. M. (2008) Effect of apolipoprotein A-V on plasma triglyceride, lipoprotein size, and composition in genetically engineered mice. *J. Lipid Res. 49*, 572–580.
28. Hauser, P. S., Raussens, V., Yamamoto, T., Abdullahi, G. E., Weers, P. M., Sykes, B. D., and Ryan, R. O. (2009) Semisynthesis and segmental isotope labeling of the apoE3 N-terminal domain using expressed protein ligation. *J. Lipid Res. 50*, 1548–1555.